FEBS Letters 589 (2015) 1847–1854

FEBS Letters

journal homepage: www.FEBSLetters.org

Phosphorylation of ULK1 by AMPK regulates translocation of ULK1 to mitochondria and mitophagy

Weili Tian [a,1], Wen Li [a,1], Yinqin Chen [b], Zeming Yan [c], Xia Huang [d], Haixia Zhuang [d], Wangtao Zhong [a], Yusen Chen [a], Wenxian Wu [a], Chunxia Lin [a], Hao Chen [a], Xiaoyan Hou [a], Liangqing Zhang [d], Senfang Sui [e], Bin Zhao [a], Zhe Hu [d,*], Longxuan Li [f,*], Du Feng [a,*]

[a] Guangdong Key Laboratory of Age-related Cardiac-cerebral Vascular Disease, Institute of Neurology, Affiliated Hospital of Guangdong Medical College, Guangdong Medical College, Zhanjiang 524001, Guangdong, China
[b] Department of Vascular Surgery, Thyroid and Mammary Gland Surgery, Guangdong Medical College, Zhanjiang 524001, China
[c] Department of Interventional Radiology, Guangdong Medical College, Zhanjiang 524001, China
[d] Department of Anesthesiology, Guangdong Medical College, Zhanjiang 524001, China
[e] State Key Laboratory of Biomembrane and Membrane Biotechnology, School of Life Sciences, Tsinghua University, Beijing 100084, China
[f] Department of Neurology, Gongli Hospital, Pudong New Area, Shanghai 200135, China

ARTICLE INFO

Article history:
Received 15 March 2015
Revised 29 April 2015
Accepted 8 May 2015
Available online 14 May 2015

Edited by Noboru Mizushima

Keywords:
Mitophagy
UNC-51 like kinase
Adenosine 5′-monophosphate (AMP)-activated protein kinase
Hypoxia
Autophagy
Mitochondria

ABSTRACT

UNC-51 like kinase (ULK1) translocates to dysfunctional mitochondria and is involved in mitophagy, but the mechanisms responsible for ULK1 activation and translocation remain unclear. Here, we found that hypoxia induces phosphorylation of ULK1 at Serine-555 by Adenosine 5′-monophosphate (AMP)-activated protein kinase (AMPK). Unlike wild-type ULK1, an ULK1 (S555A) mutant cannot translocate to mitochondria in response to hypoxia. Inhibition or knockdown of AMPK prevents ULK1 translocation and inhibits mitophagy. Finally, the phospho-mimic ULK1 (S555D) mutant, but not ULK1 (S555A), rescues mitophagy in AMPK-knockdown cells. Thus, we conclude that AMPK-dependent phosphorylation of ULK1 is critical for translocation of ULK1 to mitochondria and for mitophagy in response to hypoxic stress.

1. Introduction

Mitophagy is a process in which autolysosomes eliminate damaged mitochondria to sustain the energy balance or maintain cell survival [1–5]. At present, mitochondrial autophagy mediated by PARKIN/PINK1 is a relatively clear signal transduction pathway: In healthy mitochondria, PINK1 is constitutively expressed and imported, probably via the TIM/TOM complex, to the inner membrane where it is cleaved by presenilin-associated rhomboid-like protein (PARL) and ultimately proteolytically degraded. When the mitochondrial membrane potential is lost, PINK1 is stabilized on the outer mitochondrial membrane to recruit Parkin to depolarize the mitochondria, where Parkin ubiquitinates a subset of protein substrates to trigger mitophagy [1,4]. The autophagy initiating factor, ULK1, belonging to the Serine/Threonine kinase family, is required for autophagy induction [6–9]. ULK1 forms a complex with Atg13 and FIP200 to regulate the initial step of autophagy induction in mammalian cells. Formation of the ULK1–Atg13–FIP200 protein complex is not altered by nutrient conditions unlike its yeast counterpart, the Atg1–Atg13–Atg17 complex [10–12]. However, deletion of any of these factors does not lead to severe impairment of autophagy under starvation conditions [13]. In

Abbreviations: ULK1, UNC-51 like kinase; AMPK, Adenosine 5′-monophosphate (AMP)-activated protein kinase; FUNDC1, FUN-14 domain containing protein; mTOR, Mammalian target of rapamycin; LC3, Light chain 3

Author contributions: Du Feng and Weili Tian conceived and designed the work. Weili Tian, Wen Li, Yinqin Chen, Zeming Yan, Xia Huang, Haixia Zhuang, Wangtao Zhong, Yusen Chen, Wenxian Wu, Chunxia Lin, Hao Chen, and Xiaoyan Hou performed the experiments; Liangqing Zhang, Senfang Sui, Bin Zhao, Zhe Hu, Longxuan Li, and Du Feng analyzed the data; Weili Tian, Zhe Hu, Longxuan Li, and Du Feng wrote the paper.

* Corresponding authors at: Institute of Neurology, Affiliated Hospital of Guangdong Medical College, Zhanjiang 524001, China (D. Feng); Department of Anesthesiology, Guangdong Medical College, Zhanjiang 524001, China (Z. Hu); Department of Neurology, Gongli Hospital, Pudong New Area, Shanghai 200135, China (L. Li).

E-mail addresses: biohuzhe@hotmail.com (Z. Hu), longxuanlee2006@yahoo.com (L. Li), feng_du@foxmail.com (D. Feng).

[1] These authors contributed equally to this work.

http://dx.doi.org/10.1016/j.febslet.2015.05.020
0014-5793/

addition, even in ULK1$^{-/-}$ULK2$^{-/-}$ MEFs, long-term glucose withdrawal is able to induce autophagy [14,15], suggesting that in different cell types, the autophagy pathway responds in different ways to nutrient depletion [16].

Despite the confusion surrounding its function in starvation-induced autophagy, ULK1 plays a significant role during terminal erythroid maturation, because ULK1 null reticulocytes display delayed mitochondrial clearance during red blood cell development [17,18], indicating that ULK1 has a more specific role in mitophagy. Several proteins are involved in hypoxia-induced mitophagy in mammalian cells, including the mitophagy receptors NIX and FUNDC1 [19], or the regulatory kinases ULK1 and SRC [20–24]. In hypoxic conditions, mitochondrial outer membrane proteins like NIX and FUNDC1 are required for mitophagy by interacting with LC3 to recruit autophagic membranes. ULK1 or SRC regulates the phosphorylation status of FUNDC1 by enhancing or reducing FUNDC1-LC3 binding [17,21,22].

AMPK positively regulates autophagy under starvation conditions, while mTOR plays a negative role in this process [25–28]. However, both AMPK and mTORC1 are able to phosphorylate ULK1 and directly regulate its kinase activity. The interaction of ULK1 with AMPK is influenced by phosphorylation of ULK1 by mTORC1, and the interaction between ULK1 and mTORC1 is influenced by phosphorylation of ULK1 by AMPK [25,26,29]. Additionally, the phosphorylation of ULK1 in turn acts in a feedback loop to phosphorylate and thereby regulate AMPK or mTORC1 [30–32]. Therefore, the phosphorylation of ULK1 determines its function in autophagy. Loss of AMPK α1 or ULK1 results in aberrant accumulation of autophagy-related proteins and defective mitophagy. AMPK-phosphorylated ULK1 is required for mitochondrial homeostasis and cell survival, and connects cellular energy sensing to mitophagy [25].

We recently identified FUNDC1 as a new substrate of ULK1. It recruits ULK1 to damaged mitochondria, regulating autophagic clearance of damaged mitochondria in hypoxic conditions [21]. Nevertheless, the phosphorylation status of ULK1 during hypoxia and the mechanism that triggers mitochondrial translocation of ULK1 have yet to be revealed. Here, we found that phosphorylation of ULK1 at Serine-555 by AMPK is involved in translocation of ULK1 to mitochondria and in mitophagy.

2. Materials and methods

2.1. Antibodies and reagents

The following primary antibodies were used in this study: anti-AMPKα1 antibody (Cell Signaling Technology, #2532), anti-PRKAA1 (AMPKα) antibody (Thermo, MA5-15815), anti-phospho-AMPK α1 antibody (Cell Signaling Technology, #2535), anti-ULK1 antibody (H-240) (Santa Cruz, sc-33182), anti-Atg1/ULK1 antibody (Sigma, A7481), anti-ULK1 (D8H5) rabbit mAb (Cell Signaling Technology, #8054), anti-phospho-ULK1 (Ser757) rabbit mAb (Cell Signaling Technology, #6888), anti-phospho-ULK1 (Ser555) rabbit mAb (Cell Signaling Technology, #5869), anti-phospho-ULK1 (Ser317) rabbit mAb (Cell Signaling Technology, #12753), anti-p62/SQSTM1 antibody (MBL, PM045), anti-beta-Actin antibody (Santa Cruz, sc-47778), anti-LC3B polyclonal antibody (Sigma, L7543), anti-LC3 polyclonal antibody (MBL, PM036), anti-TIM23 (BD Biosciences, 611222), anti-TOM20 (FL-145) (Santa Cruz, sc-11415), anti-VDAC1 monoclonal antibody (Abcam, ab14734), anti-FUNDC1 polyclonal antibody (Aviva, ARP53280_P050), anti-HA Clone 16B12 monoclonal antibody (Covance, MMS-101R). Secondary antibodies used for western blotting were: HRP affinipure goat anti-mouse IgG (Earthox, E030110), HRP affinipure goat anti-rabbit IgG (Earthox, E030120) and HRP-conjugated goat anti-rabbit IgG Fc (SouthernBiotech, 4041-05). The following fluorescent secondary antibodies were obtained from Life Technologies: Alexa Fluor 488-labeled donkey anti-mouse IgG (A21202), Alexa Fluor 488-labeled donkey anti-rabbit IgG (A21206), Alexa Fluor 555-labeled donkey anti-mouse IgG (A31570), Alexa Fluor 555-labeled donkey anti-rabbit IgG (A31572). Bafilomycin A1 (50 nM, B1793) and Metformin hydrochloride (2 mM, PHR1084-500MG) were purchased from Sigma. Dorsomorphin 2HCl (1 μM, S7306) was purchased from Selleck. Protein A/G plus-agarose immunoprecipitation reagent (Santa Cruz, sc-2003), and Lipofectamine 2000 (Invitrogen, 11668027) were used according to the manufacturer's protocol.

2.2. Plasmids and siRNA

HA-AMPK and HA-ULK1 S317A were given as gifts by Prof. Kun-Liang Guan. HA-ULK1 (S555A) was gifted by Dr. Georg Ramm. HA-hULK1 (deposited by Do-Hyung Kim) was obtained from Addgene. HA-AMPK KD (kinase dead), HA-ULK1 (S555D) and HA-ULK1 (S757A) were created by site-directed mutagenesis using HA-AMPK and HA-ULK1 as the templates. Mutations were confirmed by sequencing. SiRNA sequences for AMPK α1 subunit, oligo1: 5′-CCCAUAUUAUUUGCGUGUAdTdT-3′; oligo2: 5′-GAATC CTGTGACAAGCACAdTdT-3′.

2.3. Cell culture and transfection

HeLa, ULK1 (+/+) MEFs and ULK1 (−/−) MEFs (deposited by Dr. Sharon Tooze) were cultured in DMEM (Gibco) supplemented with 10% fetal bovine serum (Hyclone) and 1% penicillin/streptomycin at 37 °C under 5% CO_2. Hypoxic conditions were achieved with a hypoxic chamber (Billups–Rothenberg) flushed with a pre-analyzed gas mixture of 1% O_2, 5% CO_2, and 94% N_2. Transfection with siRNA was performed according to the manufacturer's protocol. Plasmids were transfected into cells using Lipofectamine 2000 (Invitrogen).

2.4. Subcellular fractionation

Cells were collected and resuspended in hypotonic buffer (10 mM KCl, 210 mM sucrose, 70 mM mannitol, 1 mM EDTA, 1 mM EGTA, 1.5 mM $MgCl_2$, 10 mM HEPES; pH adjusted to 7.4 with KOH). After gentle homogenization with a Dounce homogenizer (about 50 times), cell extracts were centrifuged at 3000×g for 10 min at 4 °C. The supernatant was removed to an eppendorf tube and 100 μl was set aside in another eppendorf as the post-nuclear supernatant (PNS). The remaining supernatant was centrifuged at 10000×g for 10 min and the new supernatant was removed and set aside as the cytoplasmic fraction (Cyto). The pellet was washed twice with hypotonic buffer, resuspended in 0.5 ml hypotonic buffer, then layered on top of a step Percoll (GE Healthcare Life Science) gradient (2 ml 80%, 4.5 ml 52%, 4.5 ml 26% in a SW40 tube) which was centrifuged at 20000×g for 2 h. A 0.4 ml fraction (the mitochondrial fraction, Mito) was collected from the interface between the 26% and 52% layers and diluted with 0.8 ml hypotonic buffer. The Mito fraction was centrifuged in an eppendorf tube at 20000×g for 10 min and washed 3 times with hypotonic buffer. Samples were mixed with 100 μl 1× loading buffer and heated for 10 min at 100 °C before analyzing by western blotting.

2.5. SDS–PAGE and western blotting

Cells were lysed in lysis buffer (20 mM Tris–Cl, pH 7.5, 150 mM NaCl, 2 mM EDTA, 1.5 mM Na_3VO_4, 50 mM NaF, 10 mM β-glycerophosphate, 1% triton, phosphatase inhibitor) with 1 mM PMSF and protease inhibitor cocktail (Roche Applied Science).

Equivalent protein quantities (30 μg) were subjected to SDS–PAGE, and transferred to PVDF membranes (Millipore). Membranes were probed with the indicated primary antibodies, followed by the appropriate HRP-conjugated secondary antibodies. Immunoreactive bands were visualized with Pro-light HRP (Tiangen) or Immobilon Western Chemiluminescent HRP Substrate (Millipore). For quantitation of the bands on the immunoblot, we scanned the films and analyzed the scans using ImageJ software (NIH). Beta-actin levels were used to correct for gel loading differences.

2.6. Immunofluorescence microscopy

When the treated cells had grown to 70% confluence on a coverslip, they were washed twice with PBS (pre-warmed), and fixed with freshly prepared 4% paraformaldehyde (pre-warmed) at 37 °C for 20 min. Antigen accessibility was increased by treatment with 0.1% Triton X-100 on ice. After blocking with 2% BSA (bovine serum albumin), fixed cells were incubated with primary antibodies for 1 h at room temperature, washed with PBS, then stained with a secondary antibody for a further 1 h at room temperature. Cell images were captured with a TCS SPF5 II Leica confocal microscope. Colocalization analysis was done by ImageJ software using the "RG2B colocalization" ImageJ plugin (using default parameters). LC3 puncta were counted automatically by ImageJ.

2.7. Immunoprecipitation

After culturing under hypoxic condition for 12 h, cells were lysed in 1 ml of lysis buffer (50 mM Tris–Cl pH 7.5, 150 mM NaCl, 1 mM EDTA, 1% NP-40, 30% glycerin) containing 1 mM PMSF and protease inhibitor cocktail (Roche Applied Science) for 30 min on ice. Followed by $10000\times g$ centrifugation for 10 min, the lysates were immunoprecipitated with specific antibody and protein A/G plus-agarose immunoprecipitation reagent (Santa Cruz) overnight at 4 °C. The precipitants were then washed 5 times with lysis buffer, and the immune complexes were eluted with sample buffer containing 1% SDS for 10 min at 100 °C and analyzed by 12% SDS–PAGE.

2.8. Electron microscopy

Electron microscopy was performed as described previously [33]. Briefly, cells were fixed in 2.5% glutaraldehyde in 0.1 M sodium phosphate buffer, pH 7.4, at 37 °C for 2 h, and then dehydrated in a graded ethanol series and embedded. Approximately 70 nm ultrathin sections were mounted on copper grids. The samples were then stained and visualized using a 120 kV Jeol electron microscope (JEM-1400) at 80 kV. Images were captured using a Gatan-832 digital camera.

2.9. Statistical analysis

Assays for characterizing cell phenotypes were analyzed by Student's t-test, and correlations between groups were calculated using Pearson's test. P values <0.01 were deemed statistically significant.

3. Results

3.1. Hypoxia induces changes in ULK1 phosphorylation and promotes translocation of ULK1 to mitochondria

How is ULK1 phosphorylated in response to hypoxic conditions? We first examined the expression of ULK1 and its phosphorylation at three candidate phosphorylation sites (Ser-317, Ser-555, or Ser-757) [34]. The protein level of ULK1 is markedly elevated in response to hypoxia; however, the three phosphorylation sites are modified differently (Fig. 1A). The phosphorylation of Serine-317 and Serine-555 increases, although the latter site shows much stronger phosphorylation than the former. In contrast, phosphorylation of Serine-757 decreases sharply (Fig. 1A). In the meantime, the phosphorylation of threonine-172 in AMPK α1 also increases in responses to hypoxia, but the protein level of AMPK α1 is not significantly changed (Fig. 1A). Subcellular fractionation assays demonstrate that in hypoxic cells, a proportion of ULK1 and phosphorylated ULK1 (Ser-555) can be detected in the fraction that is enriched in mitochondrial components (Fig. 1B). Further, immunoprecipitation experiments reveal that the binding of ULK1 with AMPK α1 is much stronger in hypoxic than in normoxic conditions, while the interaction of ULK1 and mTOR is stronger in normoxic conditions (Fig. 1C). Immunofluorescence results show that mutating Ser-555 to alanine (S555A) abolishes the translocation of ULK1 to mitochondria under hypoxia. As a control, mutating Ser-757 to alanine (S757A), which removes the site phosphorylated by mTORC1, markedly affects the translocation of ULK1 (Fig. 1D and E). To be noted, the total number of ULK1 punctate has not significantly changed in cells transfected ULK1 (WT), ULK1 (S555A), or ULK1 (S757A) (Fig. 1F).

3.2. AMPK α1-dependent phosphorylation of ULK1 is critical for translocation of ULK1 to mitochondria in response to hypoxia

In order to investigate whether AMPK α1 is the critical factor for ULK1 phosphorylation and mitochondrial translocation under hypoxia, we determined the phosphorylation status of ULK1 following different treatments, including inhibition of AMPK α1 activity by the agonist Dorsomorphin 2HCl or siRNA knock-down of AMPK α1. As shown in Fig. 2A, Dorsomorphin 2HCl effectively blocks the phosphorylation of AMPK α1 at Thr-172 under hypoxic conditions. Meanwhile, the hypoxia-induced phosphorylation of ULK1 at Ser-555 and Ser-317 also vanishes completely, whereas phosphorylation of Ser-757 is not obviously changed. Similar changes in phosphorylation status are observed when the endogenous AMPK α1 is knocked down in MEF cells by siRNA. Phosphorylation of AMPK α1 at Thr-172 and ULK1 at Ser-555 and Ser-317 are abolished under hypoxia, whereas phosphorylation of ULK1 at Ser-757 decreases slightly (Fig. 2B). The protein level of ULK1 does not change after blocking AMPK α1 activity or knocking down endogenous AMPK α1 (Fig. 2B).

Immunofluorescence shows that ULK1 translocates to the mitochondria in hypoxic cells. However, after blocking the activity of AMPK α1 or knocking down the endogenous AMPK α1, ULK1 no longer translocates to the mitochondria when cells are exposed to hypoxia (Fig. 2C and D).

3.3. Ser-555 of ULK1 plays an important role in hypoxia-induced mitophagy

Next, we examined the role of ULK1 Ser-555 phosphorylation in hypoxia-induced mitophagy. Under hypoxic conditions, depletion of endogenous ULK1 inhibits degradation of mitochondrial proteins including VDAC, TOM20 and TIM23, as well as the autophagy substrate p62. Similar results were observed in ULK1 (WT) MEFs treated with Bafilomycin A1 (Baf1) under hypoxia (Fig. 3A and B). Reconstitution of exogenous ULK1 in ULK1 KO cells restores mitophagy under hypoxic conditions. Adding the ULK1 (S555A) mutant cannot restore mitophagy in hypoxic ULK1 KO cells. However, introducing the phospho-mimic mutant ULK1 (S555D) into ULK1 KO cells markedly stimulates mitophagy (Fig. 3A and B). Ultrastructure analysis by electron microscopy

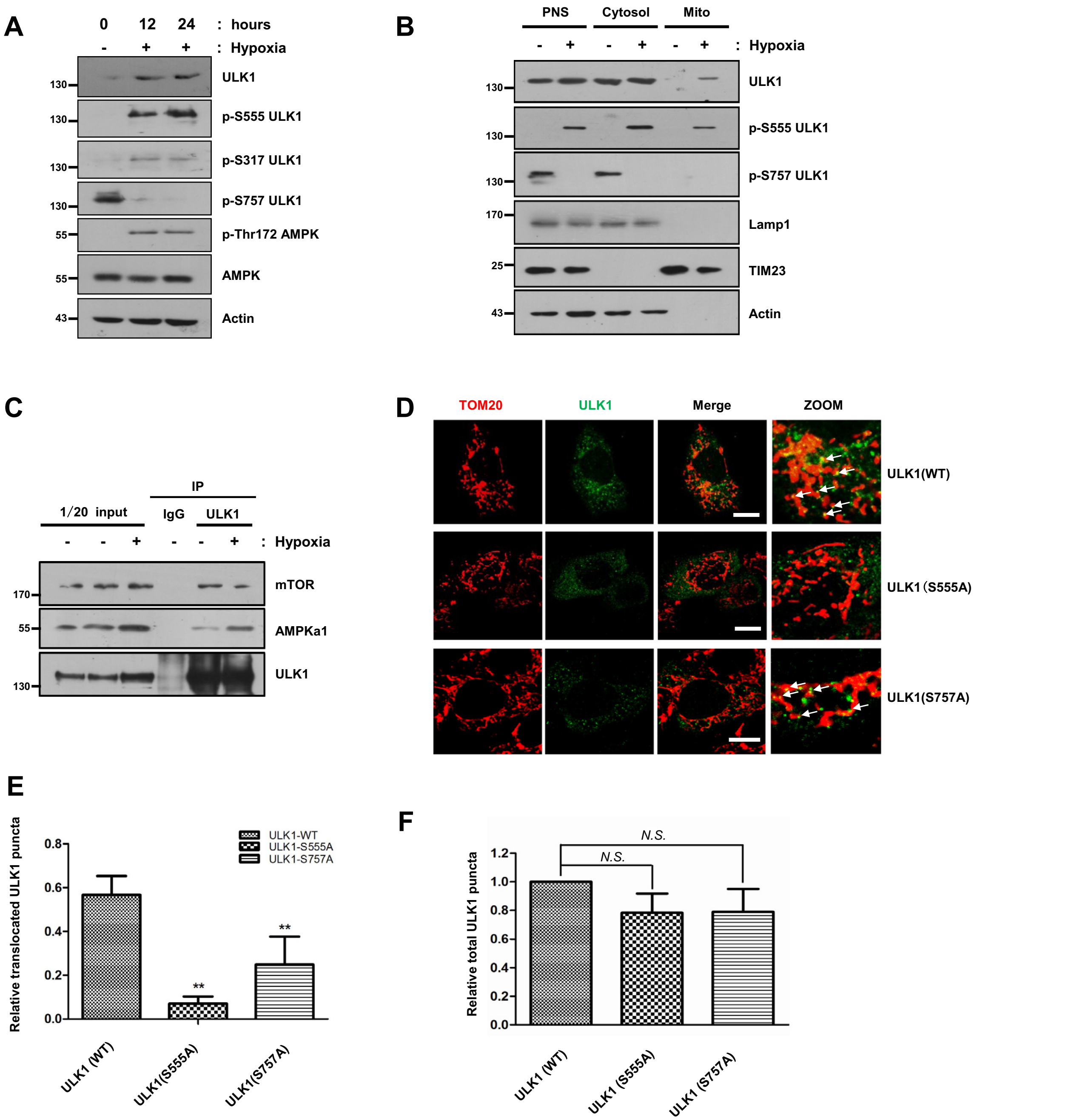

Fig. 1. Hypoxia induces changes in ULK1 phosphorylation and promotes translocation of ULK1 to mitochondria. (A) Western blot analysis of MEFs exposed to hypoxia (1% O_2) for the indicated times. Levels of indicated proteins were detected by the corresponding antibodies. (B) Immunoblots of subcellular fractions from control MEFs or MEFs that were exposed to hypoxia (1% O_2) for 12 h. PNS, post-nuclear supernatant; Cyto, cytosol; Mito, mitochondria. (C) MEFs were cultured under hypoxia for 12 h, and then cell lysates were immunoprecipitated with anti-ULK1 antibody. (D) HeLa cells were exposed to hypoxia (1% O_2) for 12 h after transfection with HA-ULK1-WT, HA-ULK1 (S555A) or HA-ULK1 (S757A), and then fixed in 4% paraformaldehyde. Cells were stained with anti-HA (mouse) and anti-TOM20 (rabbit) primary antibodies then Alexa Fluor 488-labeled donkey anti-mouse IgG and Alexa Fluor 555-labeled donkey anti-rabbit IgG secondary antibodies before analysis by immunofluorescence microscopy. Arrows indicate ULK1 puncta that colocalize with mitochondria. Bar, 10 μm. (E) Quantification of the ULK1 puncta that colocalize with mitochondria (mean = S.D.; $n = 20$ cells from three independent experiments; $^{***}P < 0.001$). (F) Quantification of the total ULK1 puncta in cells transfected with ULK1 (WT), ULK1 (S555A) or ULK1 (S757A) (Data were from three independent experiments; *N.S.* = Not Significant).

(EM) was used to compare the ability of ULK1 (S555D) and ULK1 (S555A) to mediate mitophagy in ULK1 null cells. ULK1 (S555D) restores the formation of mitochondrion-containing autophagosomes (mitophagosomes) while ULK1 (S555A) does not (Fig. 3C).

It was reported previously that during hypoxia-induced mitophagy, ULK1 phosphorylates FUNDC1 and thereby enhances the binding of FUNDC1 to LC3. Here, we found that when ULK1 was immunoprecipitated with an anti-FUNDC1 antibody, a considerable proportion was phosphorylated at Serine-555 (Fig. 3D).

3.4. AMPK α1 is required for ULK1-dependent mitophagy induced by hypoxia

To further elucidate the function of AMPK α1 and its substrate ULK1 in hypoxia-induced mitophagy, we examined normal or

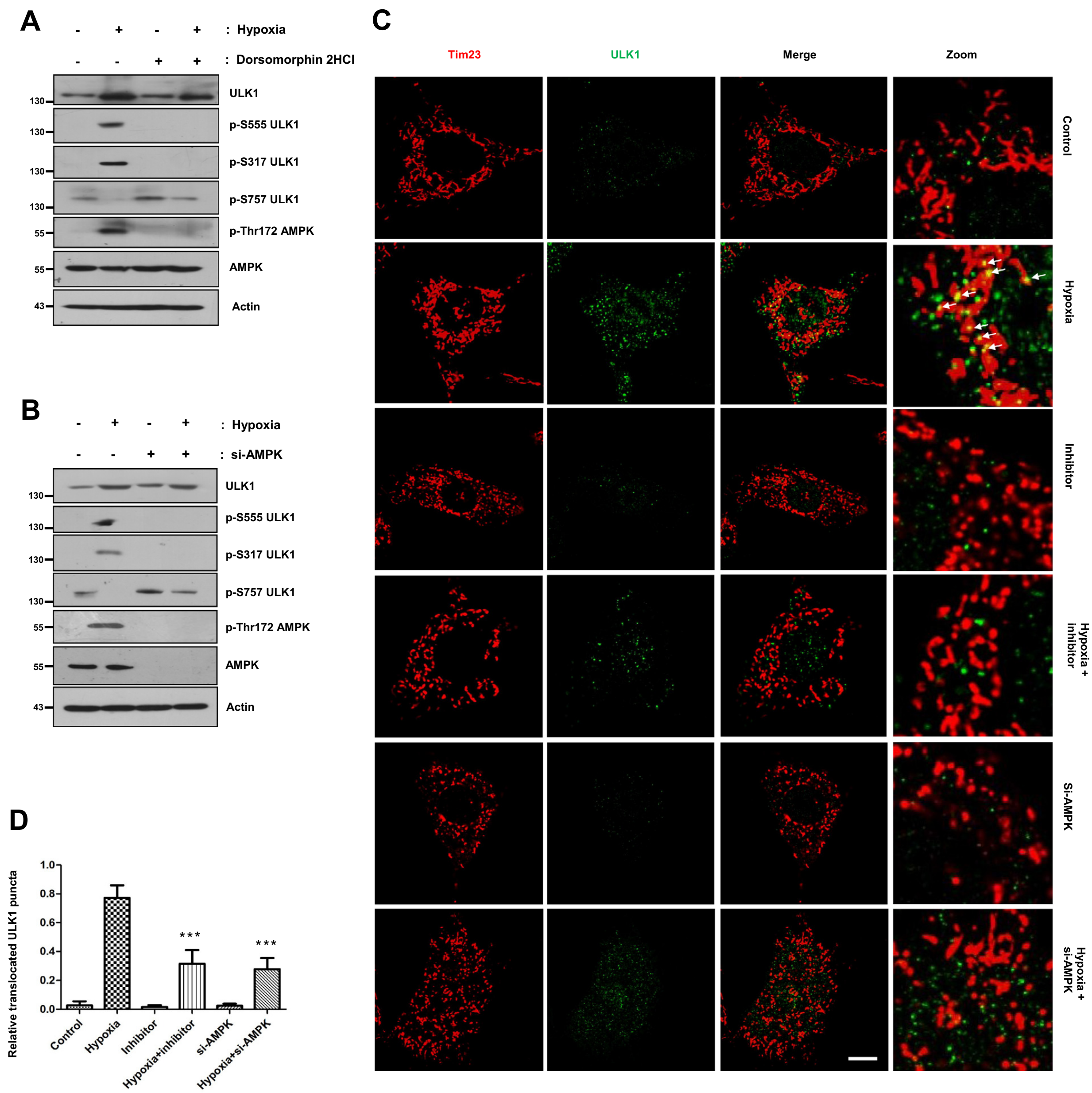

Fig. 2. AMPK α1-dependent phosphorylation of ULK1 is critical for translocation of ULK1 to mitochondria in response to hypoxia. (A) MEFs were exposed to hypoxia (1% O_2) for 12 h with or without Dorsomorphin 2HCl treatment. Cell lysates were immunoblotted for the indicated proteins. (B) MEFs were exposed to hypoxia (1% O_2) for 12 h with or without transfection of siRNA against AMPK (si-AMPK). Cell lysates were immunoblotted for the indicated proteins. (C) MEFs were cultured under hypoxia, and the activity of endogenous AMPK was inhibited with Dorsomorphin 2HCl (1 μM) or knocked down by siRNA (si-AMPK). Cells were fixed in 4% paraformaldehyde and stained with anti-TIM23 (mouse) and anti-ULK1 (rabbit) primary antibodies then Alexa Fluor 488-labeled donkey anti-rabbit IgG and Alexa Fluor 555-labeled donkey anti-mouse IgG secondary antibodies before analysis by immunofluorescence microscopy. Arrows indicate ULK1 puncta that colocalize with mitochondria. Bar, 10 μm. (D) Quantification of the ULK1 puncta that colocalize with mitochondria (mean ± S.D.; $n = 20$ cells from three independent experiments; $^{***}P < 0.001$).

kinase-dead AMPK α1 and ULK1 phosphorylation mutants in induction of mitophagy under hypoxia in AMPK α1-knockdown cells. In wild-type (WT) cells, AMPK is activated by hypoxia, as indicated by phosphorylation of Thr-172. The phosphorylation of ULK1 Ser-555 is significantly enhanced, while ULK1 Ser-757 is dephosphorylated compared to normoxia (Fig. 4A and B). In AMPK α1-knockdown cells, which do not undergo mitophagy under normoxia, phosphorylation of ULK1 Ser-757 is slightly elevated. When exogenous AMPK α1 or its constitutively phosphorylated substrate ULK1 (S555D) was reconstituted in AMPK α1-knockdown cells, the hypoxia-induced autophagic degradation of mitochondrial proteins TIM23, TOM20 and VDAC and the autophagy substrate p62 were restored. Both LC3-I and LC3-II also decreased under these conditions (Fig. 4A and B). Meanwhile, AMPK α1 kinase dead (AMPK α1 KD), wild-type ULK1 and ULK1 (S555A) all failed to rescue the mitophagy process in AMPK α1-knockdown cells exposed to hypoxia (Fig. 4A and B).

Next, we used immunofluorescence and EM to monitor the colocalization of LC3 and mitochondria and the formation of mitophagosomes. In hypoxic cells, extensive colocalization of LC3 and mitochondria was observed (Fig. 4C and D) and mitophagosomes were detected by EM (Fig. 4E). Metformin, an AMPK α1 kinase activator, is able to promote the colocalization of LC3 and mitochondria and induce mitophagosome formation even without hypoxic treatment (Fig. 4E). However, knocking down endogenous AMPK α1 or adding the AMPK inhibitor Dorsomorphin 2HCl

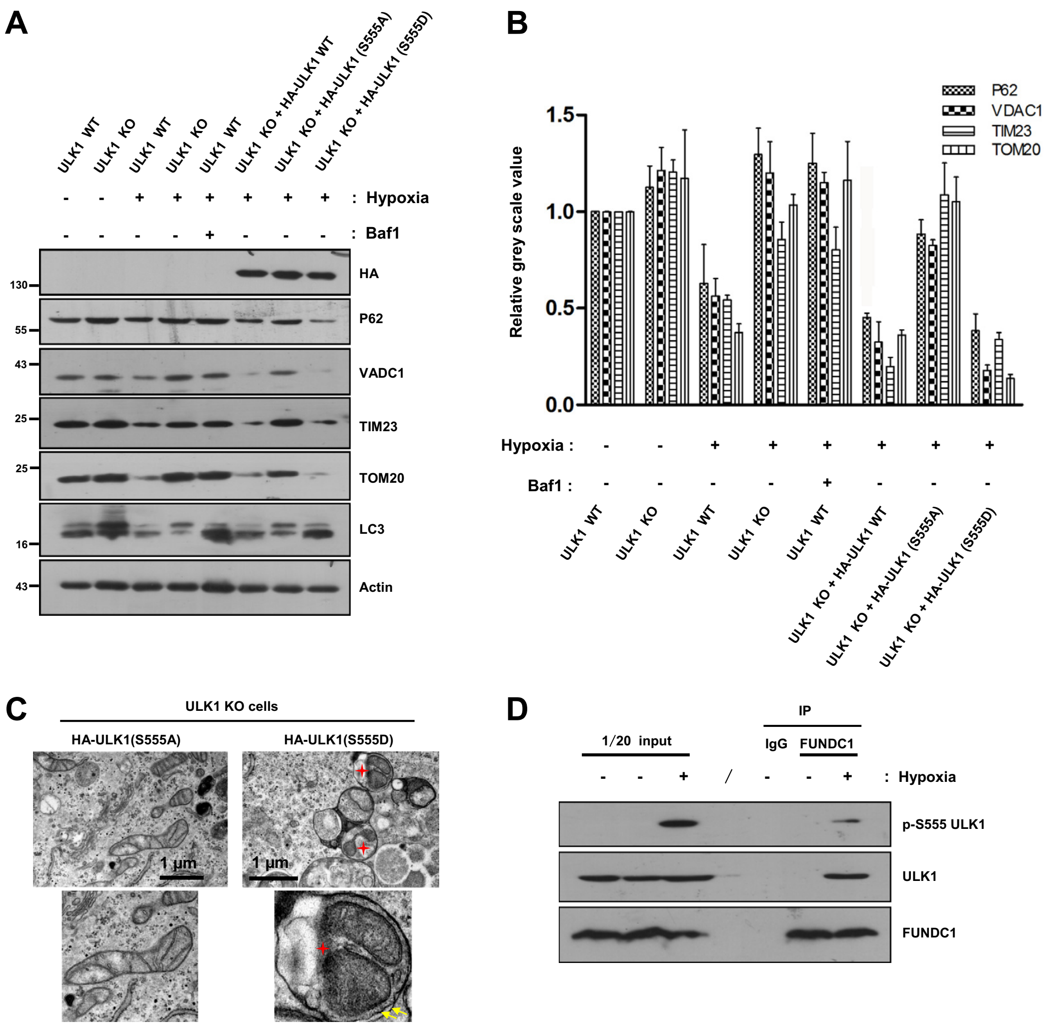

Fig. 3. Ser-555 of ULK1 plays an important role in hypoxia-induced mitophagy. (A) ULK1 (+/+) and ULK1 (−/−) cells, and ULK1 (−/−) cells transfected with HA-ULK1 WT, HA-ULK1 (S555A) or HA-ULK1 (S555D), were cultured under hypoxic (1% O_2) conditions for 12 h in the absence or presence of 50 nM Bafilomycin A1 (Baf1). Cell lysates was immunoblotted to detect the indicated proteins. (B) Quantification of the ratio of p62, VDAC1, TIM23 and TOM20 to Actin in (A). Data were from three independent experiments. (C) ULK1 (−/−) MEFs were transfected with HA-ULK1 (S555A) or HA-ULK1 (S555D), cultured under hypoxic (1% O_2) conditions for 6 h, then analyzed by electron microscopy. Red asterisks mark mitophagosomes. Yellow arrows indicate double-membraned autophagosomes. (D) MEFs were cultured under hypoxia for 12 h, and then cell lysates were immunoprecipitated with anti-FUNDC1 antibody.

inhibits the appearance of mitophagic puncta in hypoxic cells without obviously affecting the formation of single-membraned autolysosomes (Fig. 4E).

4. Discussion

AMPK is regarded as a potential candidate in mitophagy regulation because it maintains cellular energy homeostasis by sensing and manipulating energy status. It influences the erythrocyte life span by accumulating dysfunctional mitochondria and responding to reactive oxygen species (ROS) [35,36]. Defective autophagy-dependent mitochondrial clearance and accumulation of damaged mitochondria have been observed in the blood cells of AMPK α1 (−/−) mice; these abnormalities were corrected by transplantation of WT bone marrow [25]. Hypoxia can trigger AMPK α1 activation through ROS-dependent CRAC (calcium release-activated calcium) channel activation, leading to an increase in cytosolic calcium that activates the AMPK α1 upstream kinase CaMKKβ [35]. Regulation of ULK1, an autophagy initiating kinase, plays a central role in general autophagy, in particular in autophagosome formation [11]. However, recent studies indicate that it has a selective function in mitophagy upon stimulation by different environmental cues. ULK1 has been identified as the substrate of AMPK α1 which connects cellular energy sensing to mitophagy in glucose or nutrient starvation-induced autophagy [16,17,22]. Several potential ULK1 phosphorylation sites have been identified in these studies, but the dynamic changes in the phosphorylation status of ULK1 during hypoxia are not clear. In our study, hypoxia significantly induced AMPK α1 activation as indicated by phosphorylation at Thr-172 (Fig. 1A), which is consistent with AMPK activation in response to other stimuli including glucose withdrawal or energy depletion [25,26,32,35]. Phosphorylation of ULK1 at Ser-555 and Ser-317 also increased dramatically under hypoxia, while phosphorylation at Ser-757 decreased (Fig. 1A). Interestingly, the phosphorylation pattern of ULK1 under hypoxic conditions is similar to that in glucose or nutrient starvation-induced autophagy, suggesting that a common mechanism of ULK1 activation is shared between general autophagy and mitophagy [25,26,30,32,35].

The changes in phosphorylation status are possibly due to the actions of the different binding partners of ULK1 during hypoxia, since the ULK1/AMPK α1 interaction is increased in hypoxic cells while the ULK1/mTOR interaction is decreased (Fig. 1C). In

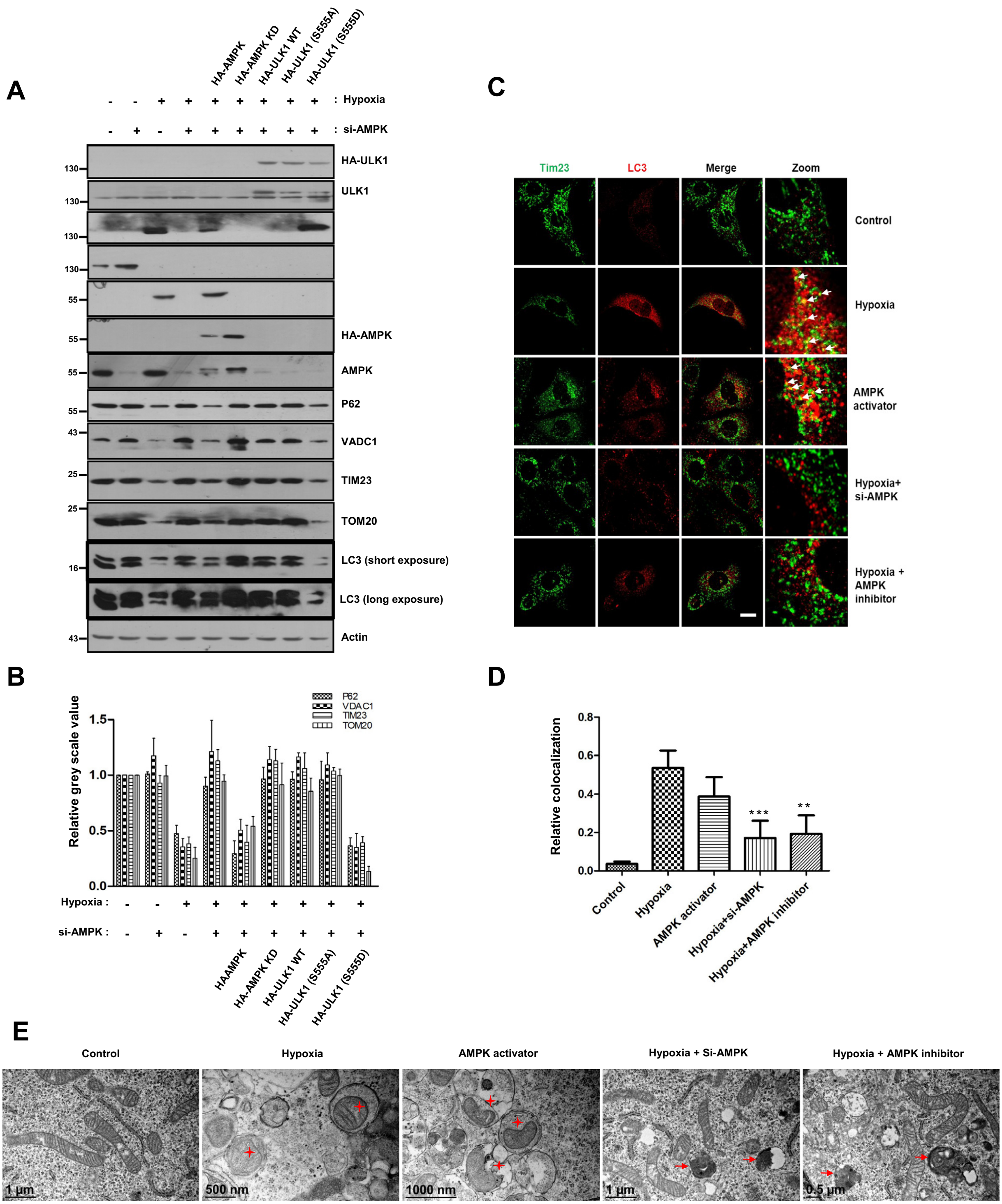

Fig. 4. AMPK $\alpha 1$ is required for ULK1-dependent mitophagy induced by hypoxia. (A) MEF cells were exposed to hypoxic conditions for 24 h, and the rescuing effect of HA-AMPK, HA-AMPK KD, HA-ULK1 WT, HA-ULK1 (S555A) or HA-ULK1 (S555D) was examined after endogenous AMPK was knocked down with si-AMPK. Cell lysates were immunoblotted for the indicated proteins. (B) Quantification of the ratio of p62, VDAC1, TIM23 and TOM20 to Actin in (A). Data were from three independent experiments. (C) MEFs were cultured under hypoxia for 6 h and treated with Dorsomorphin 2HCl (1 µM) to inhibit AMPK, si-AMPK to knock down endogenous AMPK, or Metformin (2 mM) to activate AMPK. The cells were fixed in 4% paraformaldehyde and stained with anti-TIM23 (mouse) and anti-LC3 (rabbit) primary antibodies then Alexa Fluor 488-labeled donkey anti-mouse IgG and Alexa Fluor 555-labeled donkey anti-rabbit IgG secondary antibodies before analysis by immunofluorescence microscopy. Bar, 10 µm. (D) Quantification of the translocated ULK1 puncta (mean = S.D.; $n = 20$ cells from three independent experiments; $^{**}P < 0.01$; $^{***}P < 0.001$). (E) Cells were treated as in (C), and then analyzed by electron microscopy. Red asterisks mark mitochondrion-containing mitophagosomes. Red arrows indicate autolysosomes.

mitophagy, the phosphorylation of ULK1 at Ser-555 and Ser-317 is increased, which may be due to the strengthened binding of AMPK $\alpha 1$ with ULK1 (Fig. 1C). In contrast, under normoxic conditions, the activity of AMPK is inhibited by mTORC1 binding, as shown by the absence of phosphorylation at Ser-757 of ULK1 (Fig. 1A and C).

ULK1 translocates to dysfunctional mitochondria during mitophagy initiation, yet the upstream ULK1 activator has not been reported. In our study, inhibition of AMPK $\alpha 1$ activation or silencing of AMPK $\alpha 1$ results in loss of ULK1 phosphorylation at Ser-555 and disturbs the translocation of ULK1 to mitochondria, suggesting that AMPK $\alpha1$ may be an ULK1 activator during hypoxia-induced mitophagy (Fig. 2A and B). Deletion of ULK1 retards mitophagy induction upon hypoxia treatment, while ULK1 (S555D), which mimics constitutively phosphorylated ULK1, rescues mitophagy induction in ULK1$^{-/-}$ MEFs (Fig. 3A–C). These results indicate that phosphorylation of ULK1 at Ser-555 is essential for mitophagy to proceed normally (Fig. 3A–C). We monitored the induction of mitophagy by labeling LC3 and mitochondria. Hypoxia and the AMPK $\alpha1$ activator Metformin were able to induce mitophagy, while silencing or inhibition of AMPK $\alpha1$ impaired normal mitophagy induction under hypoxia (Fig. 4). We silenced the expression of AMPK $\alpha1$ in MEFs and found that ULK1 (S555D), which mimics constitutively phosphorylated ULK1, rescues the impaired mitophagy resulting from AMPK $\alpha1$ knockdown (Fig. 4).

In conclusion, we found that AMPK $\alpha1$ phosphorylates and activates ULK1, and the activated form of ULK1 translocates to the mitochondria in hypoxia-induced mitophagy. Moreover, the ULK1 (S555D) mutant, which mimics constitutive phosphorylation of ULK1 at Ser-555 by AMPK $\alpha1$, is able to restore the impaired mitophagy resulting from AMPK $\alpha1$ silencing or inhibition. Thus, our results revealed that AMPK and ULK1 work co-operatively in mitophagy induced by hypoxia.

Disclosure of potential conflicts of interest

The authors declare that they have no conflict of interest.

Acknowledgements

We thank Isabel Hanson for editing the manuscript. We are grateful to Prof. Kun-Liang Guan for providing the HA-AMPK and HA-ULK1 S317A plasmids. We also thank Dr Georg Ramm for sending the HA-ULK1 (S555A) construct. This work was supported by the NSFC (No. 31401182, No. 31301104, No. 81171244, No. 81470405, No. 31491240358), by the Natural Science Foundation of Guangdong Province, China (2014A030313533), by the Medical Scientific Research Foundation of Guangdong Province, China (No. A2014484), by the Shanghai Natural Science Foundation of China (No. 15ZR1437200), by the Key Discipline Construction Project of Pudong Health Bureau of Shanghai (PWZx2014-08), by the Outstanding Leaders Training Program of Pudong Health Bureau of Shanghai (PWR12014-05), and by the Foundation for Distinguished Young Talents in Higher Education of Guangdong, China (2013LYM_0035).

References

[1] Youle, R.J. and Narendra, D.P. (2011) Mechanisms of mitophagy. Nat. Rev. Mol. Cell Biol. 12, 9–14.
[2] Lemasters, J.J. (2005) Selective mitochondrial autophagy, or mitophagy, as a targeted defense against oxidative stress, mitochondrial dysfunction, and aging. Rejuvenation Res. 8, 3–5.
[3] Tolkovsky, A.M. (2009) Mitophagy. Biochim. Biophys. Acta 1793, 1508–1515.
[4] Yoshii, S.R. and Mizushima, N. (2015) Autophagy machinery in the context of mammalian mitophagy. Biochim. Biophys. Acta.
[5] Feng, D., Liu, L., Zhu, Y. and Chen, Q. (2013) Molecular signaling toward mitophagy and its physiological significance. Exp. Cell Res. 319, 1697–1705.
[6] Mizushima, N. (2010) The role of the Atg1/ULK1 complex in autophagy regulation. Curr. Opin. Cell Biol. 22, 132–139.
[7] Wirth, M., Joachim, J. and Tooze, S.A. (2013) Autophagosome formation – the role of ULK1 and Beclin1–PI3KC3 complexes in setting the stage. Semin. Cancer Biol..
[8] Levine, B., Mizushima, N. and Virgin, H.W. (2011) Autophagy in immunity and inflammation. Nature 469, 323–335.
[9] Mizushima, N., Levine, B., Cuervo, A.M. and Klionsky, D.J. (2008) Autophagy fights disease through cellular self-digestion. Nature 451, 1069–1075.
[10] Hosokawa, N. et al. (2009) Nutrient-dependent mTORC1 association with the ULK1–Atg13–FIP200 complex required for autophagy. Mol. Biol. Cell 20, 1981–1991.
[11] Itakura, E. and Mizushima, N. (2010) Characterization of autophagosome formation site by a hierarchical analysis of mammalian Atg proteins. Autophagy 6, 764–776.
[12] Jung, C.H., Jun, C.B., Ro, S.H., Kim, Y.M., Otto, N.M., Cao, J., Kundu, M. and Kim, D.H. (2009) ULK–Atg13–FIP200 complexes mediate mTOR signaling to the autophagy machinery. Mol. Biol. Cell 20, 1992–2003.
[13] Hara, T., Takamura, A., Kishi, C., Iemura, S., Natsume, T., Guan, J.L. and Mizushima, N. (2008) FIP200, a ULK-interacting protein, is required for autophagosome formation in mammalian cells. J. Cell Biol. 181, 497–510.
[14] Cheong, H., Lindsten, T., Wu, J., Lu, C. and Thompson, C.B. (2011) Ammonia-induced autophagy is independent of ULK1/ULK2 kinases. Proc. Natl. Acad. Sci. U.S.A. 108, 11121–11126.
[15] Alers, S. et al. (2011) Atg13 and FIP200 act independently of Ulk1 and Ulk2 in autophagy induction. Autophagy 7, 1423–1433.
[16] Watanabe, K. and Tsubata, T. (2009) Autophagy connects antigen receptor signaling to costimulatory signaling in B lymphocytes. Autophagy 5, 108–110.
[17] Kundu, M. et al. (2008) Ulk1 plays a critical role in the autophagic clearance of mitochondria and ribosomes during reticulocyte maturation. Blood 112, 1493–1502.
[18] Honda, S., Arakawa, S., Nishida, Y., Yamaguchi, H., Ishii, E. and Shimizu, S. (2014) Ulk1-mediated Atg5-independent macroautophagy mediates elimination of mitochondria from embryonic reticulocytes. Nat. Commun. 5, 4004.
[19] Johansen, T. and Lamark, T. (2011) Selective autophagy mediated by autophagic adapter proteins. Autophagy 7, 279–296.
[20] Novak, I. et al. (2010) Nix is a selective autophagy receptor for mitochondrial clearance. EMBO Rep. 11, 45–51.
[21] Wu, W. et al. (2014) ULK1 translocates to mitochondria and phosphorylates FUNDC1 to regulate mitophagy. EMBO Rep. 15, 566–575.
[22] Liu, L. et al. (2012) Mitochondrial outer-membrane protein FUNDC1 mediates hypoxia-induced mitophagy in mammalian cells. Nat. Cell Biol. 14, 177–185.
[23] Sowter, H.M., Ratcliffe, P.J., Watson, P., Greenberg, A.H. and Harris, A.L. (2001) HIF-1-dependent regulation of hypoxic induction of the cell death factors BNIP3 and NIX in human tumors. Cancer Res. 61, 6669–6673.
[24] Sandoval, H., Thiagarajan, P., Dasgupta, S.K., Schumacher, A., Prchal, J.T., Chen, M. and Wang, J. (2008) Essential role for Nix in autophagic maturation of erythroid cells. Nature 454, 232–235.
[25] Egan, D.F. et al. (2011) Phosphorylation of ULK1 (hATG1) by AMP-activated protein kinase connects energy sensing to mitophagy. Science 331, 456–461.
[26] Kim, J., Kundu, M., Viollet, B. and Guan, K.L. (2011) AMPK and mTOR regulate autophagy through direct phosphorylation of Ulk1. Nat. Cell Biol. 13, 132–141.
[27] Dunlop, E.A. and Tee, A.R. (2013) The kinase triad, AMPK, mTORC1 and ULK1, maintains energy and nutrient homoeostasis. Biochem. Soc. Trans. 41, 939–943.
[28] Hardie, D.G. (2014) AMPK: positive and negative regulation, and its role in whole-body energy homeostasis. Curr. Opin. Cell Biol. 33C, 1–7.
[29] Alers, S., Loffler, A.S., Wesselborg, S. and Stork, B. (2012) Role of AMPK-mTOR-Ulk1/2 in the regulation of autophagy: cross talk, shortcuts, and feedbacks. Mol. Cell. Biol. 32, 2–11.
[30] Loffler, A.S. et al. (2011) Ulk1-mediated phosphorylation of AMPK constitutes a negative regulatory feedback loop. Autophagy 7, 696–706.
[31] Dunlop, E.A., Hunt, D.K., Acosta-Jaquez, H.A., Fingar, D.C. and Tee, A.R. (2011) ULK1 inhibits mTORC1 signaling, promotes multisite Raptor phosphorylation and hinders substrate binding. Autophagy 7, 737–747.
[32] Egan, D., Kim, J., Shaw, R.J. and Guan, K.L. (2011) The autophagy initiating kinase ULK1 is regulated via opposing phosphorylation by AMPK and mTOR. Autophagy 7, 643–644.
[33] Feng, D., Zhao, W.L., Ye, Y.Y., Bai, X.C., Liu, R.Q., Chang, L.F., Zhou, Q. and Sui, S.F. (2010) Cellular internalization of exosomes occurs through phagocytosis. Traffic 11, 675–687.
[34] Bach, M., Larance, M., James, D.E. and Ramm, G. (2011) The serine/threonine kinase ULK1 is a target of multiple phosphorylation events. Biochem. J. 440, 283–291.
[35] Mungai, P.T., Waypa, G.B., Jairaman, A., Prakriya, M., Dokic, D., Ball, M.K. and Schumacker, P.T. (2011) Hypoxia triggers AMPK activation through reactive oxygen species-mediated activation of calcium release-activated calcium channels. Mol. Cell. Biol. 31, 3531–3545.
[36] Jiang, S., Park, D.W., Stigler, W.S., Creighton, J., Ravi, S., Darley-Usmar, V. and Zmijewski, J.W. (2013) Mitochondria and AMP-activated protein kinase-dependent mechanism of efferocytosis. J. Biol. Chem. 288, 26013–26026.